

A SINGLE STAGE POWER CONDITIONING OF EXTENDED BOOST QUASI Z-SOURCE INVERTER FOR PV APPLICATIONS

N.Hemalatha Dr.R.Seyezhai

Ph.D. Scholar, Department of EEE, SSN College of Engineering, Kalavakkam, India
Mobile:+91-7299915974,Email:rnhemaa@gmail.com

Associate Professor, Department of EEE, SSN College of Engineering, Kalavakkam, India
Mobile:+91-9894968847,Email: seyezhair@ssn.edu.in

Abstract: Modern renewable power generation systems require smart power converters of high efficiency for power conversion. In standalone and grid connected PV systems, the power conditioning unit should be able to provide high voltage gain and boosting capability. This paper presents a new type of power conditioning unit for the photovoltaic power generation systems. The extended q-ZSI provides an effective power conversion technology for interfacing of photovoltaic systems in a single stage. For standalone and grid connected PV systems, the extended boost q-ZSI provides high voltage boost and high input voltage gain with reduced voltage stress across the switching devices. In this paper, two topologies of extended boost q-ZSI namely modified capacitor assisted extended boost quasi-ZSI(MCAEB q-ZSI) and modified diode assisted extended boost q-ZSI(MDAEB q-ZSI) has been analyzed and compared with its voltage gain and voltage boost property. The SIMULINK model of both the topologies has been built in MATLAB/ SIMULINK. The experimental prototype model for the three phase modified capacitor assisted extended boost q-ZSI was developed and the results are validated with the simulation results.

Keywords: Modified Diode Assisted (MDAEB q-ZSI), Modified Capacitor Assisted (MCAEB q-ZSI), Boost Factor(B)

1. Introduction

Energy harvesting from the photovoltaic power generation systems is one of the promising renewable energy technology in recent years to meet the energy demand in most of the developing countries. The photovoltaic power generation systems need a power conditioning unit with the high input voltage gain to match the voltage difference and to compensate the variations in the output voltage of the PV panel [1]. For PV applications, the two stage of power conversion technology with an intermediate cascaded arrangement of the converter system increases the complexity of the power circuit and the design of the controller. Such an

intermediate arrangement needs a number of power switches resulting in the increase in the cost and space requirement. Recently the power converters for interfacing of renewable energy systems in a single stage has been proposed in the literature[2-3]. The new power converters of the extended q-ZSI can provide a single stage of power conversion for grid connected and stand alone systems by providing improved boost factor, high voltage gain and high efficiency [4-5].

In literature, the concept of extending the voltage gain of the conventional q-ZSI without increasing the number of switches has been proposed [6]. In this paper, two types of extended boost quasi-Z-source inverter topologies categorized as modified diode assisted and modified capacitor assisted extended boost q-ZSI has been analyzed for its performance[7]. The effective topology for PV applications has been identified based on the voltage boost, voltage gain, voltage stress comparison between the two topologies. A critical analysis on operating voltages of capacitors in the impedance network, ripples of the impedance network elements, the harmonic profile has been presented with the simulation results. The theoretical results are validated with the simulation and the experimental results.

2. Mathematical Modelling of PV panel

PV cells are grouped together into PV modules which are further connected in a parallel-series configuration to form PV panel. The interfacing of PV panel with the single stage extended boost q-ZSI is performed with the mathematical modeling of the solar panel [8]. The modeling of PV module was performed based on the electrical specifications given by the open circuit voltage V_{oc} :36.73V, short-circuit current I_{sc} :8.63A. These specifications are tested under the conditions of insolation of 1 kW/m² and cell temperature of 25°C. The following equations illustrate

the step by step procedure for the modeling of PV module in MATLAB/ Simulink. The subsystem model shown in the Fig.1. is used to convert the PV module operating temperature given in degree centigrade to Kelvin.

The equation for the temperature conversion is given below as

$$T_a = T_{opt} + 273 \quad (1)$$

Where

T_{opt} is the module operating temperature (25°C)

T_a is the module operating temperature in Kelvin.

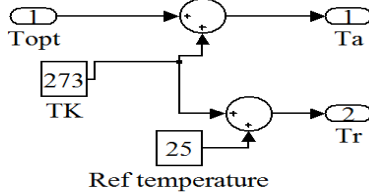


Fig.1. Subsystem for Temperature Conversion

The subsystem model used to find the photon current of the PV module is shown in the Fig.2. The equation of the photon current of the PV module is given by

$$I_p = [I_{sc} + K_{sc}(T_a - T_r)] * \lambda / 1000 \quad (2)$$

Where

I_{sc} is the short circuit current 8.63A

T_r is module reference temperature 25°C

λ is the PV module illumination 1000 (W/m2)

K_{sc} is the short-circuit current temperature co-efficient = 0.0017A / °C

The subsystem model used to calculate the reverse saturation current of the diode is shown in Fig.3. The equation for the module reverse saturation current (I_{rs}) of the diode is given by

$$I_{rs} = I_{sc} / [\exp(qV_{oc} / N_s k A T_a) - 1] \quad (3)$$

Where

V_{oc} is the open-circuit voltage (36.7V)

K is Boltzmann constant = 1.3805×10^{-23} J/K

q is Electron charge = 1.6×10^{-19} C

N_s is the number of cells connected in series(60)

T_a is the module operating temperature in Kelvin

A is an ideality factor = 1.6

The subsystem to calculate the module saturation current is shown in Fig.4. The equation for the module reverse saturation current (I_o) is given by

$$I_o = I_{rs} \left[\frac{T_a}{T_r} \right]^3 \exp \left[\frac{q^* E_{g0}}{Bk} \left\{ \frac{1}{T_r} - \frac{1}{T_a} \right\} \right] \quad (4)$$

Where

I_{rs} =reverse saturation current of diode

E_{g0} is the band gap for silicon = 1.1eV

B is an ideality factor = 1.6

The subsystem to calculate the diode current is shown in Fig.5. The equation for the diode current (I_d) is given by

$$I_d = I_o \left[\exp \left\{ \frac{q^* (V_{PV} + I_{PV} R_s)}{N_s A k T} \right\} - 1 \right] \quad (5)$$

Where V_{PV} is output voltage of a PV module (V)

I_{PV} is output current of a PV module (A)

N_s is number of cells in series (36)

R_s is series resistance of a PV module

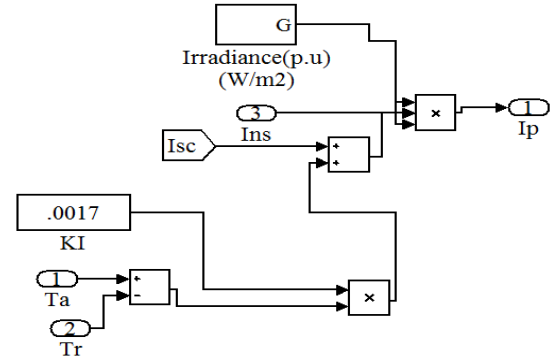


Fig.2. Subsystem for Module Photon Current

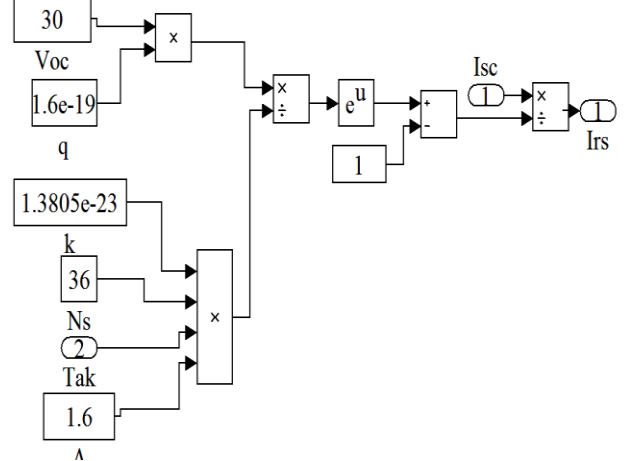


Fig.3. Subsystem for Module Reverse Saturation Current

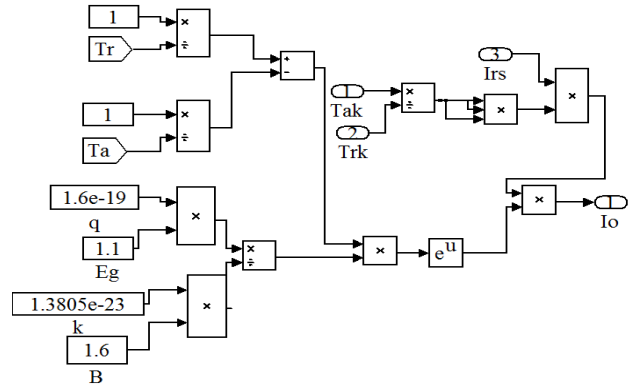


Fig.4 Subsystem for Module Saturation Current

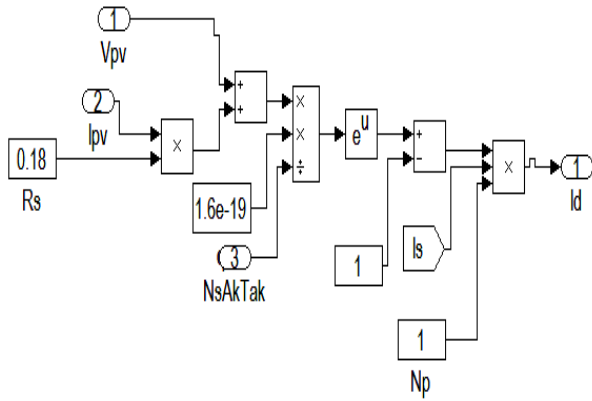


Fig.5. Subsystem for Diode Current Equation

The subsystem to calculate the shunt current is shown in Fig.6.

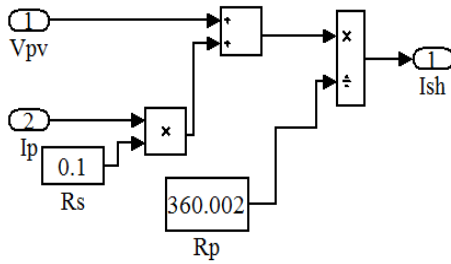


Fig.6. Subsystem for Shunt Current Equation

The subsystem to calculate the load current is shown in Fig. The equation for the load current (I_{pv}) is given by

$$I_{pv} = N_p * I_p - N_p * I_0 \left[\exp \left\{ \frac{q * (V_{pv} + I_{pv} R_s)}{N_s A k T} \right\} - 1 \right] \quad (6)$$

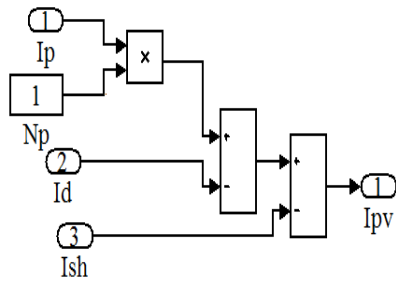


Fig.7. Subsystem for Load Current Equation

All the subsystem models are interconnected to get the SIMULINK PV model as shown in Fig.8. The subsystem for plotting the characteristics of PV panel is shown in Fig.9. The I-V and P-V output characteristics of PV panel are plotted and is shown in Fig.10. and Fig.11. This SIMULINK PV model takes irradiation, operating temperature in Celsius and module voltage as input and gives the output current I_{PV} and output voltage V_{PV} .

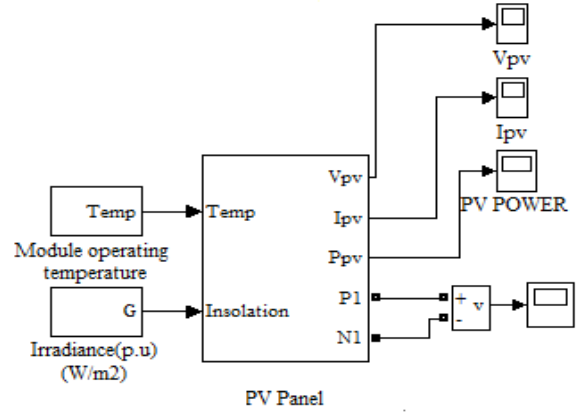


Fig.8. SIMULINK PV panel model

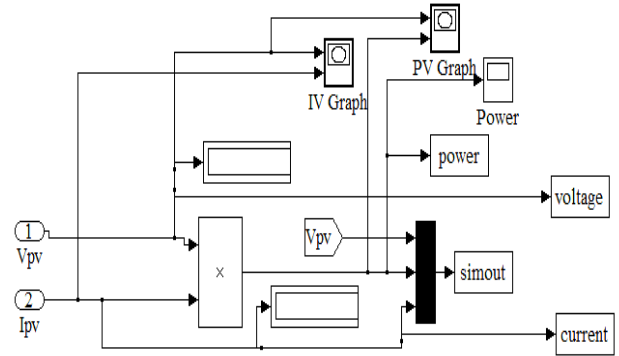


Fig.9. Subsystem for PV Characteristics

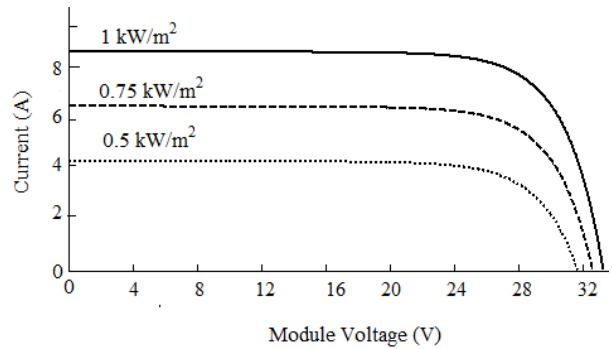


Fig.10. I-V characteristics of PV panel for Different Insolation Level

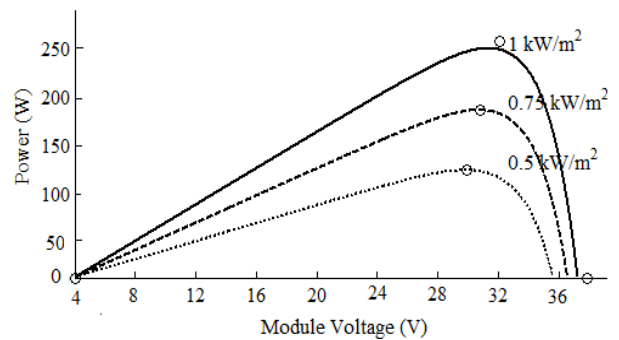


Fig.11. P-V characteristics of PV panel for Different Insolation Level

3. Topology Analysis of Extended Boost q-ZSI

The extended boost quasi Z source acts as the power conditioner unit for interfacing with the PV panel. The following topics discuss the two topologies of extended boost q-ZSI like MDAEB q-ZSI and MCAEB q-ZSI. The novel topology should be analyzed for PV applications.

3.1 Circuit Analysis of MCAEB q-ZSI

In MCAEB q-ZSI, the unique LC and diode impedance network used for boosting the DC link voltage was designed by adding one diode (D2), an inductor (L3) and capacitors (C3 and C4) to the traditional q-ZSI. The connection points of the capacitors C2 and C3 are interchanged so that the operating voltage of the capacitor C3 was reduced by more than five times as compared to its basic topology CAEB q-ZSI. It also shows that the operating voltages of the capacitors C2 and C4 are equalized to the same voltage thereby reducing its component ratings and the capacitor voltage ripple[9]. Such a unique LC impedance network is connected between the source and the inverter to attain the voltage boost and inversion in a single stage. This unique LC and diode impedance network connected to the inverter bridge change the operation of the circuit, allowing the shoot-through state which boosts the dc link voltage. This network indeed will effectively protect the circuit from damage when two devices of the same leg get shorted.

The proposed topology of modified capacitor assisted extended boost q-ZSI (MCAEB q-ZSI) is presented in Fig.12. It has a common property of the continuous input current conduction. It gives the reduced stress of the input voltage source for the demanding applications as power conditioners for solar panels.

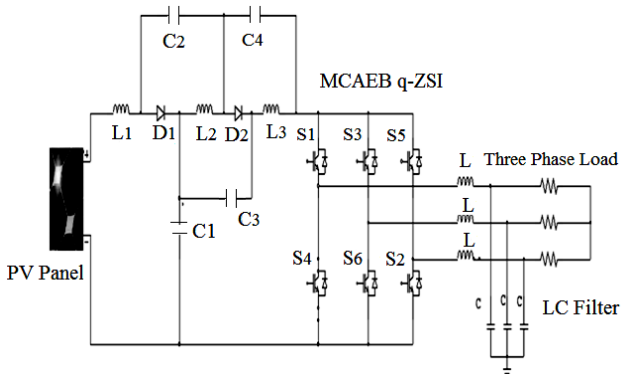


Fig.12. PV Connected MCAEB q-ZSI

The equivalent circuits for the active state and the shoot through the state are shown in Fig.13 and Fig.14.

During the shoot through the state, diodes D1 and D2 are reverse biased. The inductors L1, L2, L3 are getting charged and the energy is either transferred from the source to inductors L1, L2, L3 or from the capacitor to inductors L1, L2, L3 while the capacitors are getting discharged. During this state, there is a voltage boost in the dc link voltage. During the active state, the diodes D1 and D2 are forward biased. The inductors will be discharging and the capacitors are getting charged.

Let V_s =Input Voltage from PV panel

M_a =Modulation Index

V_d = DC link voltage

D_s =Shoot through duty ratio

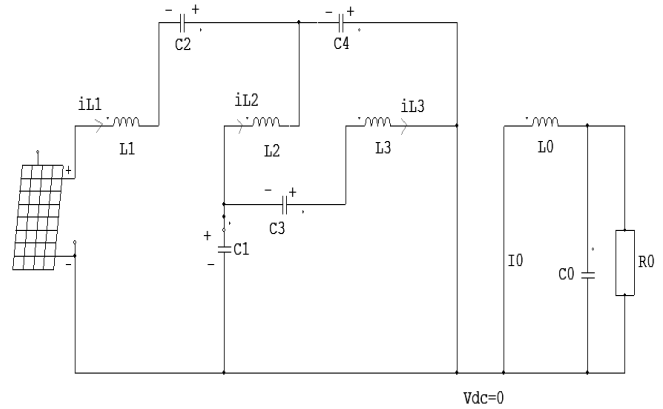


Fig.13. Equivalent circuit in shoot-through state

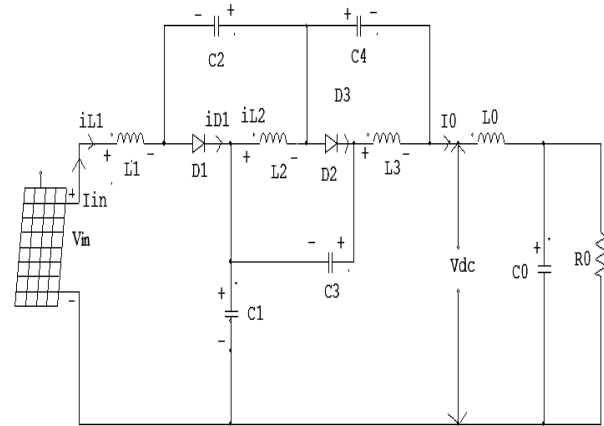


Fig.14. Equivalent circuit in active state

The operating voltages of the capacitors are given as

$$V_{C2} = V_{C3} = V_{C4} = V_s (D_s) / (1 - 3D_s) \quad (7)$$

$$V_{C1} = V_s (1 - 2D_s) / (1 - 3D_s) \quad (8)$$

The peak value of DC-link Voltage is

$$V_d = V_{C1} + V_{C2} + V_{C4} \quad (9)$$

The boost ratio of the input voltage is

$$B = V_s / V_d \quad (10)$$

3.2 Circuit Analysis of MDAEB q-ZSI

In MADEB q-ZSI, the unique LC and diode impedance network are designed by adding of one capacitor (C3), one inductor (L3) and two diodes (D2 and D3) to the traditional q-ZSI. Further by interchanging the connection points of the capacitor C3, the operating voltage of the capacitor C3 was reduced by more than five times as compared to its basic topology DAEB q-ZSI[10]. The proposed topology of modified diode assisted extended boost q-ZSI (MDAEB q-ZSI) was analyzed for PV applications and are presented in Fig.15.

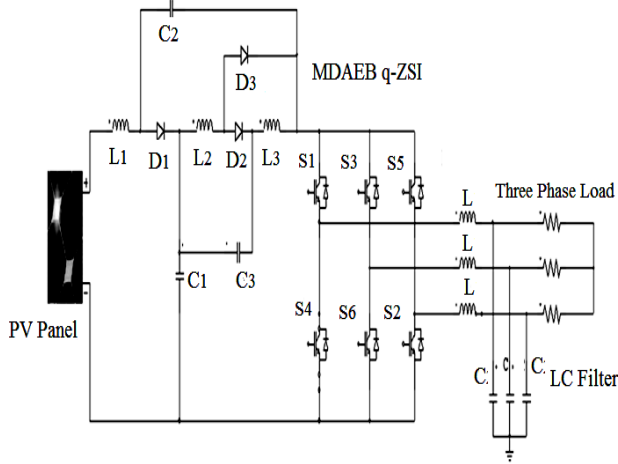


Fig.15. PV Connected MDAEB q-ZSI

The equivalent circuits of the MCAEB q-ZSI for the shoot-through and the active states are shown in Fig.16. and 17. During the shoot through the state, diodes D3 is conducting and the diodes D1, D2 are in blocking state. During this state, there is a voltage boost in the dc link voltage. During the active state, the diode D3 is in blocking state and the diodes D1 and D2 are in conducting state. The inductors will be discharging and the capacitors will be charging.

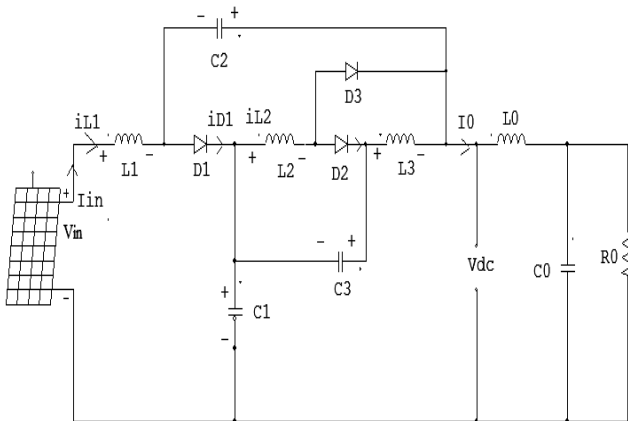


Fig.16. Equivalent circuits in non-shoot through state

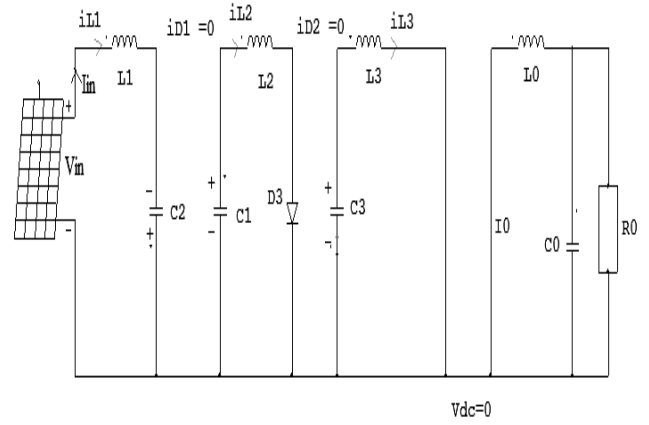


Fig.17. Equivalent circuit in shoot-through state

The peak value of DC-link Voltage is

$$V_d = V_{C1} + V_{C2} \quad (11)$$

The boost ratio of the input voltage is

$$B = V_s / V_d \quad (12)$$

$$B = 1 / (D_s^2 - 3D_s + 1)$$

4. Analytical Comparison of MDAEB q-ZSI and MCAEB q-ZSI

Analytical parameters of both the topologies were analyzed and compared for their performance. In demanding applications as power conditioners for solar panels, MCAEB q-ZSI can produce increased boost factor, reduced voltage ripple across the capacitors.

4.1 Analytical Comparison for boost factor B

For demanding applications of PV systems, high voltage gain with high boost factor is needed. Theoretical comparison of voltage boost properties between the topologies are tabulated for various modulation indices as shown in Table 1. When examined for the same shoot through duty ratio of 0.167, it is observed that MCAEB topology can produce boost factor B=2 which is slightly higher than MDAEB topology.

Table 1
Theoretical comparison of Boost Factor

Shoot through duty ratio(Ds)	MCAEB q-ZSI Boost Factor (B)	MDAEB q-ZSI Boost Factor (B)
0.3	10	5.26
0.25	4	3.25
0.2	2.5	2.25
0.167	2.0	1.5
0.05	1.6	1.11

4.2 Comparison for Operating Voltages of Capacitors in Impedance Network

The operating voltages of the capacitors in the LC impedance network have an impact on the voltage ripples across the capacitors. The voltage stress across the device gets reduced when the operating voltage across the capacitors get decreased. Thus the component rating of the capacitors and inductors in the impedance network will get reduced.

Table 2

Theoretical comparison of operating voltages of capacitors

Capacitor Voltages(V)	Capacitor Voltages (MCAEB q-ZSI)	Theoretical Values(V)
V _{C1}	$V_s(1-2D_s)/(1-3D_s)$	40
V _{C2}	$V_s * D_s / (1-3D_s)$	10
V _{C3}	$V_s * D_s / (1-3D_s)$	10
V _{C4}	$V_s * D_s / (1-3D_s)$	10

Table 2. shows the theoretical comparison of operating voltages of capacitors across the impedance network of MCAEB topology. This table illustrates that the operating voltage of capacitor C₃ in the impedance network is reduced to 10V and the capacitor voltages of C₂ and C₄ are equalized to the same value of 10V.

Table 3

Theoretical comparison of operating voltages of capacitors

Capacitor Voltages(V)	Capacitor Voltages (MDAEB q-ZSI)	Theoretical Values(V)
V _{C1}	$V_s * (D_s^2 - 2D_s + 1) / (D_s^2 - 3D_s + 1)$	40
V _{C2}	$V_s * (2D_s - D_s^2) / (D_s^2 - 3D_s + 1)$	16
V _{C3}	$V_s * (D_s - D_s^2) / (D_s^2 - 3D_s + 1)$	12

In the case of MCAEB q-ZSI by changing the interconnection points of C₃ would reduce the operating voltages of capacitors to five times of its basic topology [10].

Thus the component sizing of capacitors is reduced to the value of 185μF thereby reducing capacitor voltage ripples. When the theoretical comparison was made between the topologies, MCAEB q-ZSI features increased boost factor B for the same value of shoot-through duty cycle (D_s) than MDAEB q-ZSI.

5.Component Sizing of Inductors and Capacitors

The component sizing of inductors and the capacitors in the impedance network will limit the voltage ripple on the inverter during the active states

and the current ripple during the shoot through states[11]. The inductors L₁, L₂, L₃ in the impedance network will have the same values and are calculated based on the parameters such as switching frequency $f_s: 10\text{KHZ}$, input power rating of PV panel $P_{in}: 250\text{watts}$, input voltage from the PV panel $V_{in}: 30\text{V}$, shoot through duty ratio $D_s: 0.167$ and the average value of the inductor current ripple .

$$L_1 = (V_{c3} * D_s) / (0.2 * f * I_{L, av}) \quad (12)$$

$$L_1 = D_s * (V_{in}) / (0.2 * f * P) * (1 - D_s) / (1 - 3D_s) \quad (13)$$

$$L_1 = L_2 = L_3 \quad (14)$$

By substituting the values, $L_1 = L_2 = L_3 = 65\mu\text{H}$

The voltage ripple on the inverter during active states can be reduced by 3% at the peak power, the capacitance of capacitors C₁, C₂, C₃, and C₄ in the impedance network can be calculated as by the equation is given below.

$$C_1 = (0.2 * P * D_s) / (0.03 * V_{in} * V_{dc} * f) \quad (15)$$

$$= P * D_s * (1 - 3D_s) / (0.015 * V_{2in} * f)$$

$$C_1 = C_2 = C_3 \quad (16)$$

By substituting the values $C_1 = C_2 = C_3 = C_4 = 180\mu\text{F}$

Thus the design considerations of the inductors and the capacitors will effectively reduce the component sizing in the impedance network.

6. PV Panel interfacing with Extended Boost q-ZSI

The theoretical assumptions are validated with the simulation results with the help of Simulink model of extended boost q-ZSI using MATLAB. The PV interfaced MCAEB q-ZSI Simulink model is shown in the Fig.16 and the simulation parameters are presented in Table 4. The pulse generation unit and the gating pulse pattern are shown in Fig.17. and Fig.18.

Table 4

Simulation Parameters

	Simulation Parameters	Ratings
Solar Panel Rating	PV Panel Power	250 Watts
	V _{oc} , I _{sc}	36.73V, 8.63A
	V _{mpp} , I _{mpp}	30.6V, 8.14A,
Z Network Component	Panel output voltage	30.6V
	Inductors L ₁ , L ₂ , L ₃ & r _L	65μH
	Capacitors C ₁ , C ₂ , C ₃ & r _C	180μF
Filter Component	Filter Inductance	5mH
	Filter Capacitance	220 μF
	Switching Frequency(fs)	10KHZ
	Inverter Frequency	50HZ

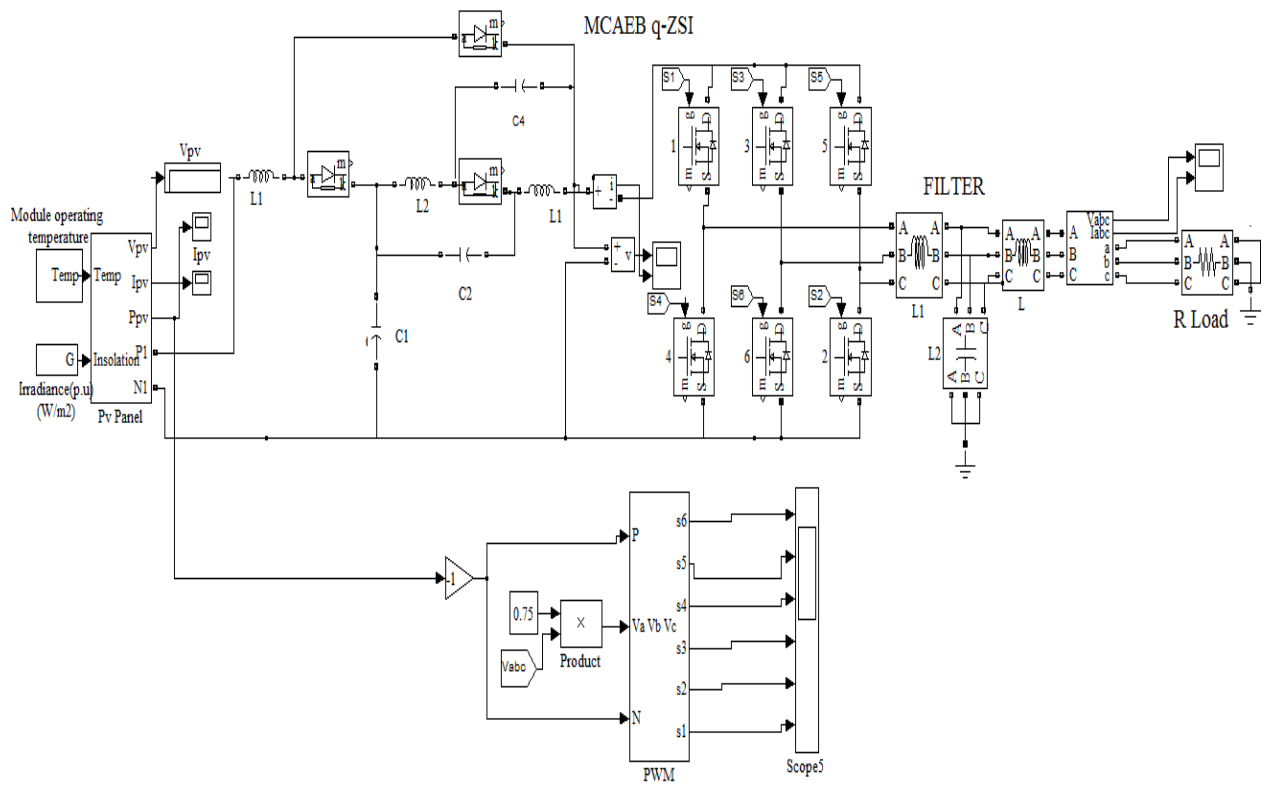


Fig.16.PV Connected MCAEB q-ZSI

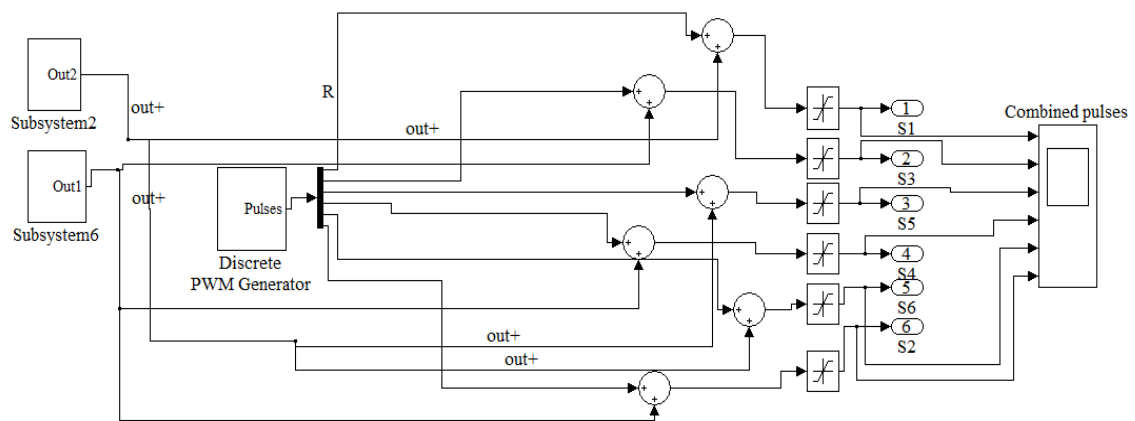


Fig.17.Pulse Generation

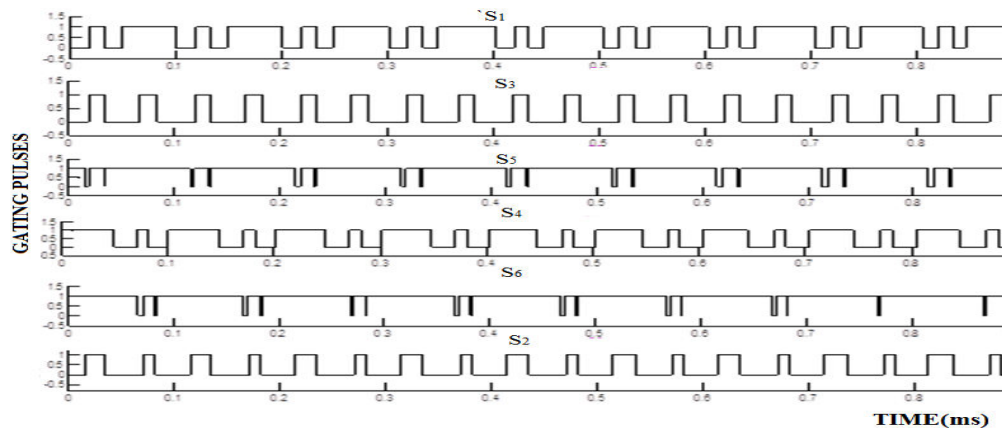
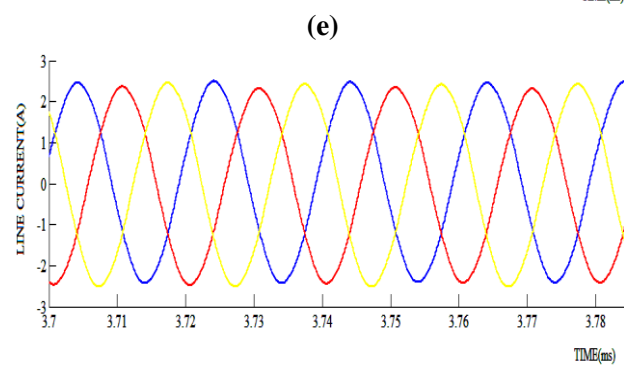
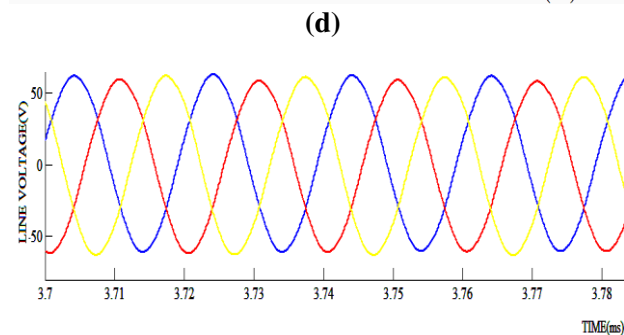
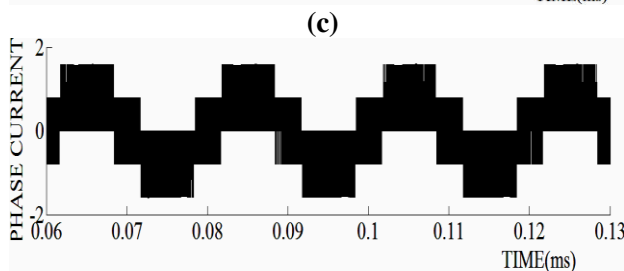
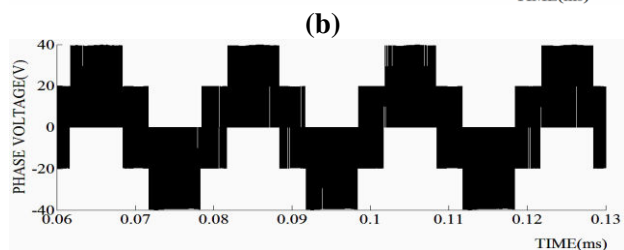
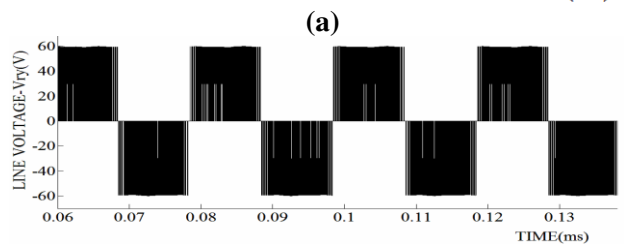
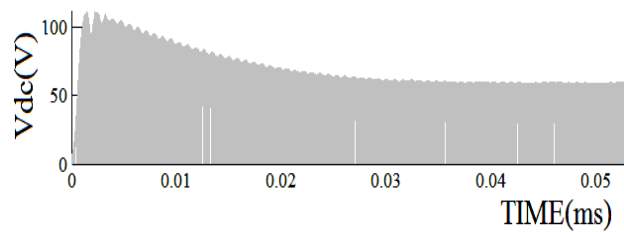
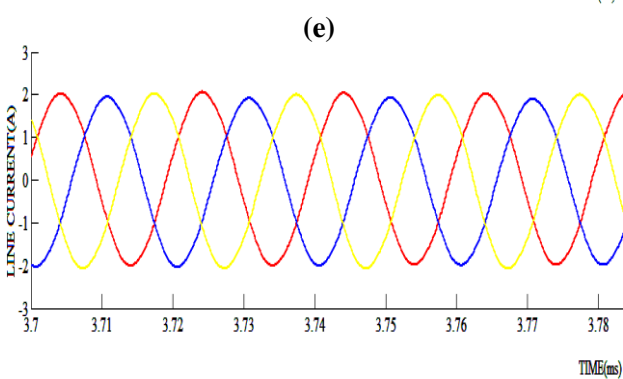
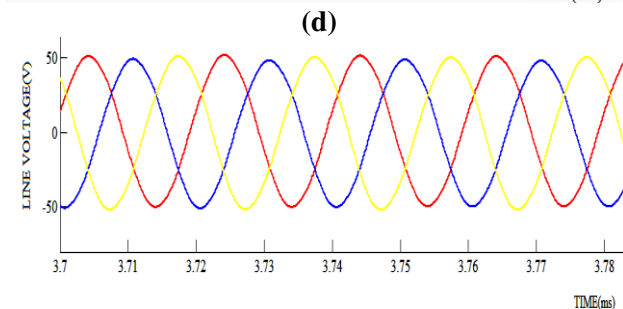
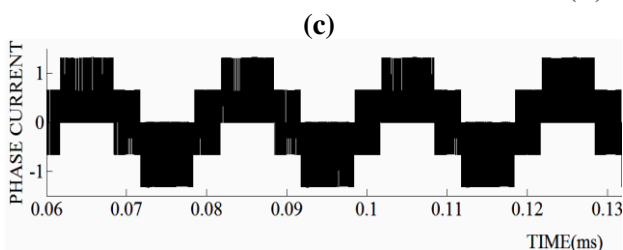
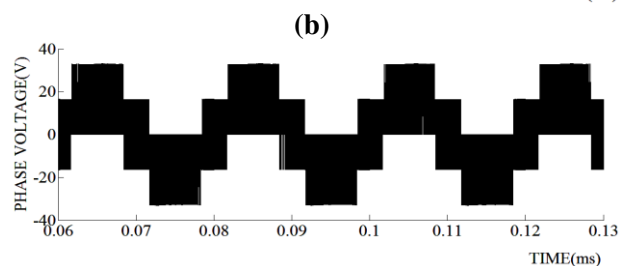
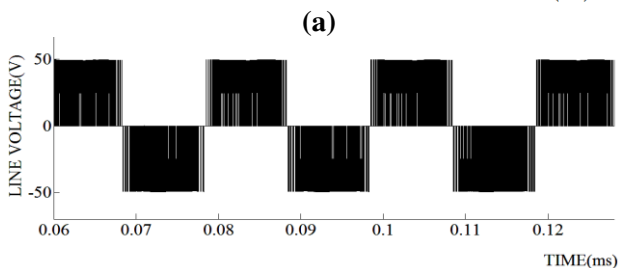
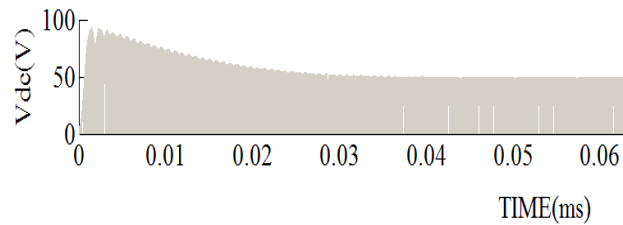


Fig.18.Gating Pulse Pattern



(f)

Fig.19. Simulation Results of MCAEB q-ZSI
(a)DC Link Voltage (b)Line Voltage (c)Phase Voltage (d) Line current without filter (e)Line Voltage with filter (f) Line current with Filter



(f)

Fig.20. Simulation Results of MDAEB q-ZSI
(a)DC Link Voltage (b)Line Voltage (c)Phase Voltage (d) Line current without filter (e)Line Voltage with filter (f) Line current with Filter

The simulation results are shown in Fig.19. and Fig.20. It represents the boost voltage, line voltage, line current and phase voltage with and without a filter for MCAEB and MDAEB q-ZSI. It is clear from the Fig.19 a. that MCAEB q-ZSI is able to provide boost voltage of 60V for Ma:0.833 which is comparatively higher than MDAEB q-ZSI. Table 5 illustrates the comparative study of both the topologies based on their simulation results.

Table 5
Comparative Result Analysis

Parameters	Notations	MDAEB q-ZSI	MCAEB q-ZSI
Shoot through	D_s	0.167	0.167
Modulation Index	M_a	0.833	0.833
Boost Factor	B	1.89	2
Boost Voltage	V_d	56V	60V
DC Link Voltage	V_{dc}	56V	60V
Line-Line Voltage	V_{L-L}	56V	60V
RMS Line Voltage	$V_{L-L(rms)}$	45.7V	48.98V
Phase Voltage	V_{ph}	32.33V	34.64V
RMS Phase Voltage	$V_{ph(rms)}$	26.39V	28.28V

The proposed topology should provide high boost factor for demanding power required for PV applications. The variation of boost factor B for various modulation indices is shown in Fig.21. It is inferred when the Simulink model is executed for the shoot through duty cycle D_s :0.167, MCAEB topology is able to produce twofold of its input voltage from the PV panel.

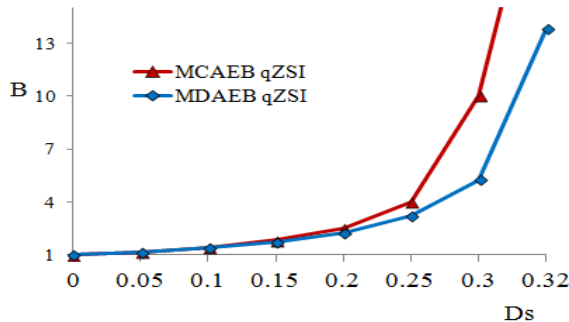


Fig.21.Boost Factor Comparison

As the power conditioner for PV systems, MCAEB q-ZSI should be able to provide high voltage gain when interfaced with PV systems. The voltage gain comparison between topologies was tabulated as presented in Table 6. Fig.22. shows the variation of voltage gain for different values of modulation indices. The simulation results infer that when voltage gain comparison was made between topologies for $M_a=0.833$, MCAEB q-ZSI is able to produce voltage gain $G=2.7$ which is comparatively higher than

MDAEB q-ZSI.

Table 6
Voltage Gain Comparison

Modulation Index (M_a)	MDAEB q-ZSI Voltage gain (G)	MCAEB q-ZSI Voltage gain (G)
0.7	3.684	7
0.75	2.4	3
0.833	1.716	2.7
0.85	1.487	1.5
0.95	1.061	1.121

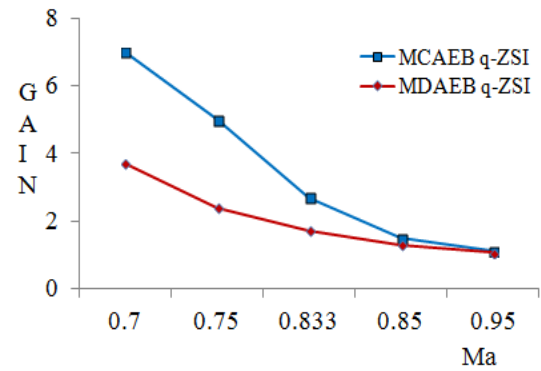


Fig.22. Voltage Gain Comparison

The inductor current ripple and the capacitor voltage ripple were calculated across the impedance network of the proposed topologies and is presented as shown in Fig.23. and Fig.24. It is inferred from the simulation result that MCAEB q-ZSI is able to provide reduced current ripple and voltage ripple across the inductors and the capacitors in the impedance network. Table 7 and Table 8 illustrates the variation of inductor current ripple and capacitor voltage ripple for various modulation indices.

Table 7
Inductor Current Ripple across L1

Modulation Index (M_a)	MCAEB q-ZSI Current Ripple(A)	MDAEB q-ZSI Current Ripple(A)
0.7	0.2538	0.415
0.75	0.1794	0.219
0.8	0.1244	0.127
0.85	0.1088	0.114
0.9	0.0824	0.077

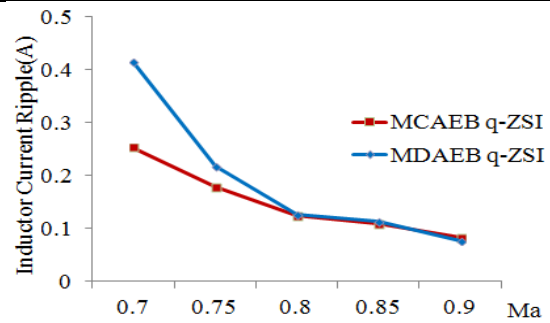


Fig.23.Inductor Current Ripple

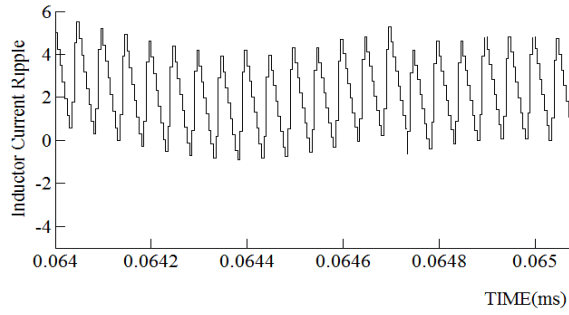


Fig.24.Inductor Current Ripple of MCAEB q-ZSI

Table 8
Capacitor Voltage Ripple across C1

Modulation Index (Ma)	MCAEB q-ZSI Voltage Ripple (V)	MDAEB q-ZSI Voltage Ripple (V)
0.75	0.0172	0.0210
0.8	0.0236	0.0312
0.85	0.0254	0.0392
0.75	0.0172	0.0210
0.8	0.0236	0.0312

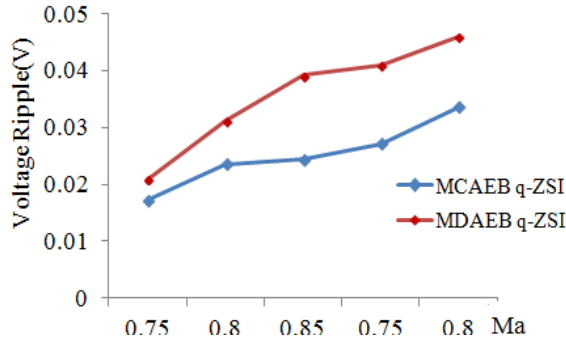


Fig.24.Capacitor Voltage Ripple

The voltage stress comparison between the two topologies was compared with different modulation indices and is presented in Fig.25. Table 9 brings in the voltage stress comparison between the two proposed topologies.

Table 9
Voltage Stress Comparison

Modulation Index (Ma)	MDAEB q-ZSI Voltage Stress	MCAEB q-ZSI Voltage Stress
0.75	133.73	43.68
0.8	79.8	40.74
0.85	55.27	31.45
0.75	41.45	28.98
0.8	23.56	22.26

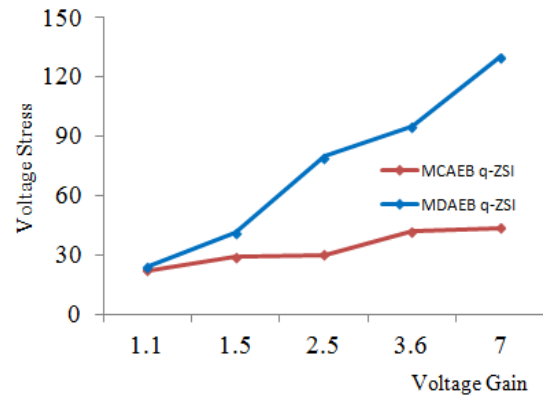


Fig.25.Voltage Stress Comparison

MCAEB q-ZSI has reduced voltage stress across the switches due to reduced voltage and current ripple in the impedance network. THD comparison is shown in Fig.26. MCAEB q-ZSI has reduced value of THD which informs that the output voltage

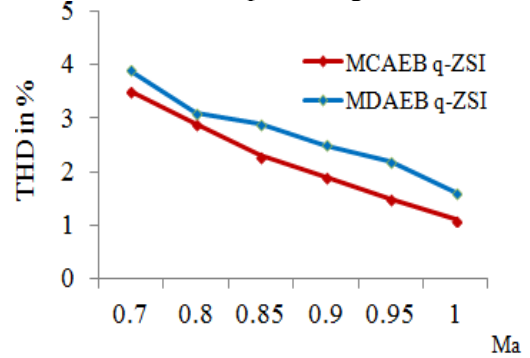


Fig.26. THD Comparison

When the performance parameters like boost factor, voltage gain, voltage stress, inductor current ripple, capacitor voltage ripple and THD were compared between the two topologies of extended boost q-ZSI, it is found that MCAEB q-ZSI has excellent results than MDAEB q-ZSI. The performance parameters were compared in Table 10.

Table 10
Performance Result Analysis

Parameters	Notations	MDAEB q-ZSI	MCAEB q-ZSI
Shoot through	D_s	0.167	0.167
Modulation Index	M_a	0.833	0.833
Boost Factor	B	1.89	2
Voltage Gain	G	1.86	2.7
Voltage Stress	V_s	55.27	31.45
Total Harmonic Distortion	THD	4.5%	2.8%
Current Ripple		0.112A	0.102A
Voltage Ripple		0.0372V	0.0214V

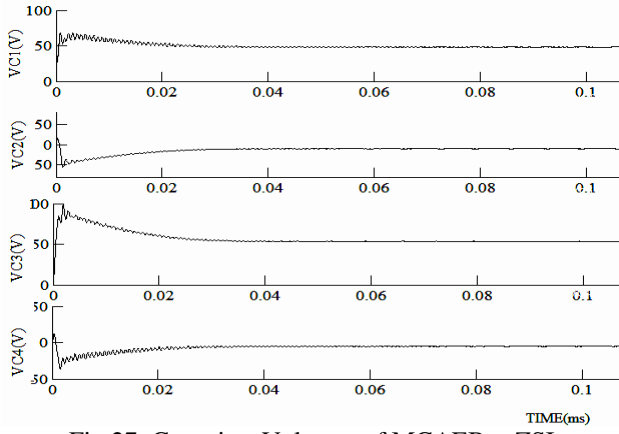


Fig.27. Capacitor Voltages of MCAEB q-ZSI

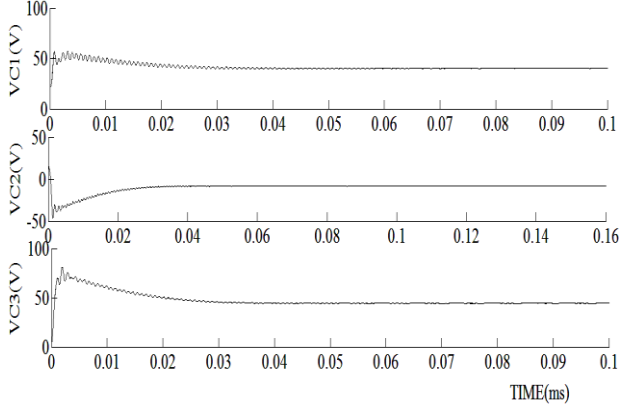


Fig.28. Capacitor Voltages of MDAEB q-ZSI

From the Fig.27. and Fig.28.it is clear that the working voltage of capacitor C_4 are reduced to more than six times and the working voltages of C_3 and C_2 are equalized in the case of MCAEB q-ZSI.This, in turn, reduces the component sizing of capacitors in the impedance network. From the simulation results, it is clear that MCAEB q-ZSI is the preferred topology for PV applications.

7. Experimental Results

To order to verify the theoretical and simulated results, an experimental prototype of PV connected MCAEB q-ZSI was proposed and is shown in Fig.16.The prototype was implemented by connecting 250 watts PV panel supplying 30V DC input to the power circuit The Z-source parameters used in the impedance network for the hardware setup are $L_1 = L_2 = L_3 = 65\mu\text{H}$ and $C_1 = C_2 = C_3 = C_4 = 180\mu\text{F}$. The Z-network in the power circuit is designed using electrolytic type capacitors and inductors. The extended boost q-ZSI will invert to 60V AC output. The inverted AC voltage will be utilized by the load side where the demand will be met depending on the requirement of generation.

A photograph of the hardware prototype is shown in the Fig.29. The inverter switches in the power circuit are built with IRF840 power MOSFET which is a fast

switching N-channel enhancement mode MOSFET.

The control circuit is built with a dsPIC30F4011 controller. The main Features of the dsPIC30F4011 controller are enhanced programmable flash memory and data EEPROM memory, self-reprogrammable under software control, programmable code protection. The gate drive circuit TLP250 is used produce high current gate drive for a power circuit and also acts as an isolation circuit preventing high voltages from affecting the system.

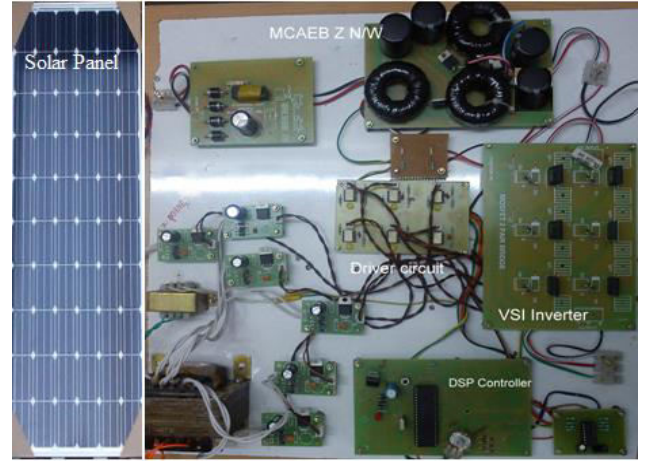


Fig.29. Experimental Setup

The input voltage from the PV Panel is assumed to be 29V and is represented in Fig 30.For PV applications the proposed topology can be operated in a continuous current conduction mode with the input current never dropping to zero. This is one of the best features of this topology towards PV applications.

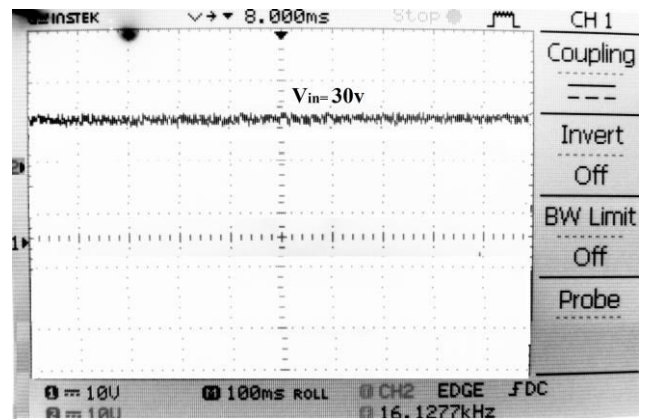


Fig.30. DC Input Voltage

The shoot through pulses generated during the switching sequence of the three phase inverter was shown in Fig.30.For producing the boost voltage twice fold of the input voltage, the shoot through duty cycle for MCAEB q-ZSI should be 0.167 with the modulation index of 0.833.

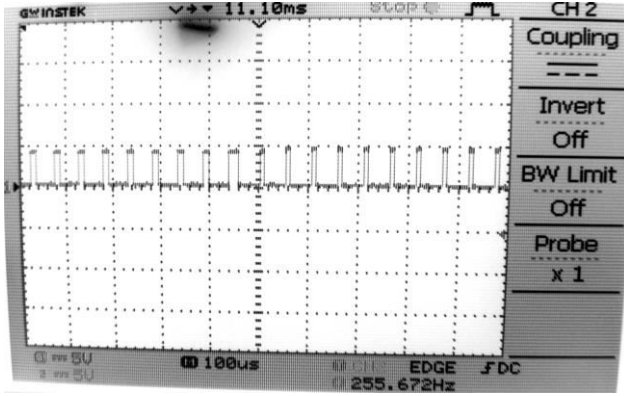
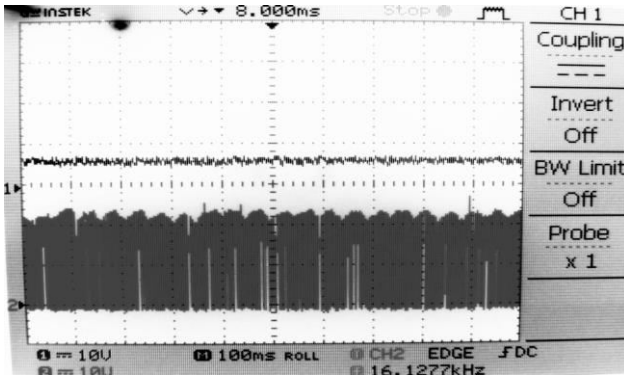


Fig.30. Shoot through Pulses

The boost voltage produced across the impedance network of the proposed topology is shown in Fig.31. From the hardware results it is clear that for the DC input voltage 30V, the proposed topology is able to produce 58V for the shoot through duty cycle of 0.25ms.



The proposed topology is able to maintain the DC link voltage across the impedance network which makes it most preferable for PV applications.

The operating voltage of the capacitor C_3 for a shoot through a period of 0.25ms is shown in Fig.31.

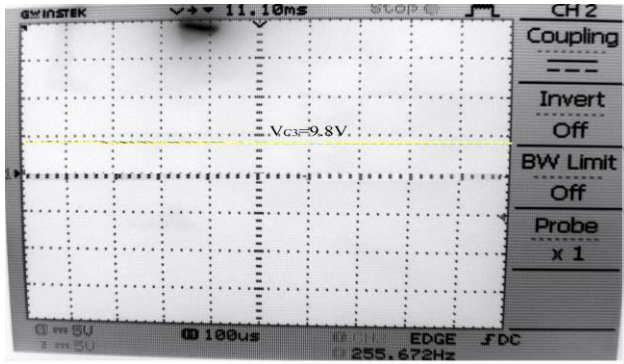


Fig.31. Capacitor Voltage of MCAEB q-ZSI

The results show that the working voltage of C_3 in the impedance network is reduced to 9.2V and the working voltages of C_2 and C_4 are equalized to 9.2V.

thereby reducing the ripples in the impedance network which reduces the voltage stress across the switching devices improving the voltage boost to 58V and voltage gain to the value of $G=3$.

The phase voltage and the line voltage of the proposed topology are shown in Fig.32. and Fig.33.

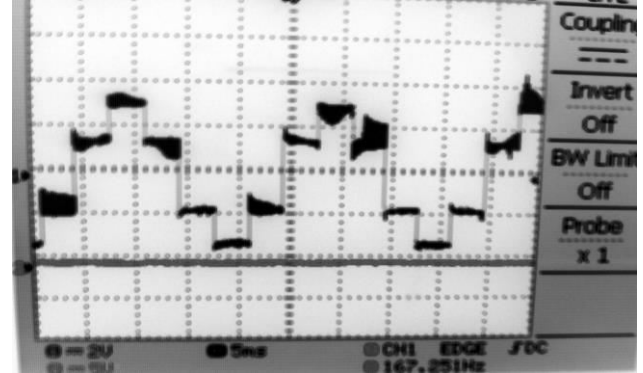


Fig.32. Output Phase Voltage

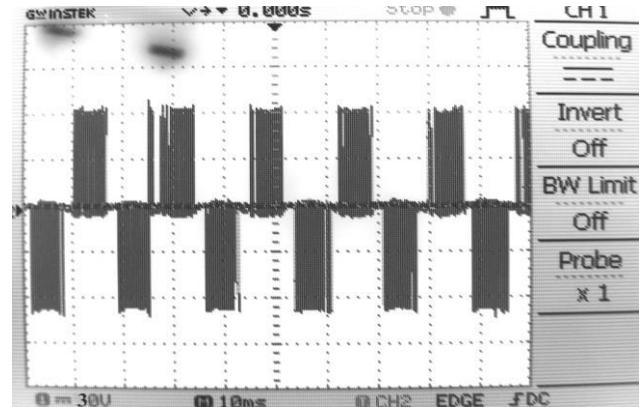


Fig.33. Line Voltage

From the hardware results, the line voltage is 58 V and the phase voltage of the proposed topology is nearly 33V for the conditions given. The experimental results of MCAEB q-ZSI were validated with the simulated and theoretical results to conclude that it is a preferable topology for PV systems.

8. Conclusion

In this paper, a detailed steady-state analysis of the two types of topologies of extended boost quasi-Z-source inverter namely MDAEB and MCAEB q-ZSI were performed. The detailed analysis on voltage boost, voltage gain, voltage stress, harmonic profile performance brings out that MCAEB q-ZSI provides a better spectral quality of the output when compared with MDAEB q-ZSI. The proposed topology also ensures the continuous input current for PV applications. MCAEB q-ZSI is the most promising topology for the single stage power conditioning of grid connected and stand alone applications of PV systems.

ACKNOWLEDGMENT

The authors wish to thank the management of SSN institutions for providing the computational facilities to carry out this work.

References

- [1] Anderson, J., Peng, F.Z: *Four Quasi-Z-Source Inverters*. In: Proceedings of IEEE Power Electronics Specialists Conference PSEC2008,15-19, June 2008, Rhodes, p.2743– 2749.
- [2] Yuan Li., Joel Anderson., Fang Z. Peng., Dichen Li: *Quasi-Z-Source Inverter for Photovoltaic Power Generation Systems*. In: Proceedings of Applied Power Electronics Conference and Exposition APEC 2009, 15-19 Feb ,2009, Washington,p.918-924.
- [3] Badin, R., Huang, Y., Peng, F.Z., Kim, H.G: *Grid Interconnected Z-Source PV System*. In: Proceedings of IEEE Power Electronics Specialists Conference PESC2007, 17-21 June 2007, Orlando,p.2328-2333.
- [4] Yi Huang., Miaosen Shen., Fang Z. Peng., Jin Wang: *Z-Source Inverter for Residential Photovoltaic Systems*. In: IEEE Transactions on Power Electronics ,Vol.21,No.6,1776-1782, November 2007.
- [5] Jong-Hyoung Park., Heung-Geun Kim., Eui-Cheol Nho., Tae-Won Chun., Jaeho Choi: *Grid-connected PV System Using a Quasi-Z-source Inverter*.In: Applied Power Electronics Conference and Exposition APEC 2009, Feb 15-19, 2009, Washington,p.925-929.
- [6] Gajanayake, J., Luo, F.L., Gooi, H.B., So, P.L., Siow, L.K: *Extended boost Z-source inverters*. In: Proceedings of Energy Conversion Congress and Exposition ECCE2009,20-24 Sept 2009, San Jose CA, p. 3845-3845.
- [7] Chandana Jayampathi Gajanayake., Hoay Beng Gooi Lip Kian Siow: *Extended-Boost Z-Source Inverters*. In: IEEE Transactions on Power Electronics, Vol.25, No.10, p.2642-2652,May 2010.
- [8] Shah Arifur Rahman., Rajiv Varma, K., Tim Vanderheide: *a Generalised model of a photovoltaic panel*. In: IET Renewable Power Generation, Vol.8, No.3,p.217-229,2014.
- [9] Vinnikov, D., Roasto, I., Jalakas, T: *Comparative Study of Capacitor-Assisted Extended Boost qZSIs Operating in CCM*. In: Proceedings of IEEE Baltic Electronic Conference BEC,4-6 Oct 2010, Tallinn, p.297-300.
- [10] Seyezhai, R., Hemalatha, N: *Modified Diode Assisted Extended Boost For PV Applications*. In: Scientific Research Circuits and Systems, Vol.7, No.10,p.3271-3284, August 2016.
- [11] Rajakaruna, S., Jayaywickrama, R.L: *Designing Impedance Network of Z-Source Inverters*. In: Proceedings of the 7th international Power Engineering Conference IPEC2005, 29Nov-2Dec,2005, Singapore, p.324-357.
- [12] Yuan Li., Shuai Jiang., Cintron-Rivera, J.G., Fang Zheng Peng: *Modeling and Control of Quasi-Z-Source Inverter for Distributed Generation Applications*. In: IEEE Transactions on Industrial. Electronics.,Vol.60, p.1532–1541,2013.
- [13] Rostami, H., Khaburi, D. A.: *Voltage Gain Comparison of Different Control Methods of the Z-Source Inverter*. In: Proceedings of International Conference on Electrical and Electronics Engineering ELECO2009, 05-08 Nov 2009, Bursa, Turkey, p.268-272.
- [14] Adamowicz, M., Strzelecki, R., Vinnikov, D: *Cascaded Quasi-Z-Source Inverters for Renewable Energy Generation Systems*. In: Proceedings of 10th International Conference on Ecologic Vehicles and Renewable Energies EVER'10, March 2010, Monaco,p.25-28.
- [15] Thangaparakash, S., and Krishnan A: *Current mode integrated control technique for Z-source inverter-fed induction motor drives*. In: Journal of Power Electronics, Vol. 10, No. 3, pp. 1-8, 2010.
- [16] Husodo, B.Y., Anwari, M., Ayob, S.M., Taufik: *Analysis and Simulations of Z-Source Inverter Control Methods*. In: Proceedings of International Power Engineering Conference IPEC2010,27-29 Oct 2010, Singapore.p.699-704.

